AIDA-2020-NOTE-2019-004

AIDA-2020

Advanced European Infrastructures for Detectors at Accelerators

Scientific/Technical Note

Fibre test benches for the characterisation of media for calorimeters with optical readout

E. Auffray

et al

20 December 2018

The AIDA-2020 Advanced European Infrastructures for Detectors at Accelerators project has received funding from the European Union's Horizon 2020 Research and Innovation programme under Grant Agreement no. 654168.

This work is part of AIDA-2020 Work Package **14: Infrastructure for advanced calorimeters**.

The electronic version of this AIDA-2020 Publication is available via the AIDA-2020 web site <http://aida2020.web.cern.ch> or on the CERN Document Server at the following URL: <http://cds.cern.ch/search?p=AIDA-2020-NOTE-2019-004>

Grant Agreement No: 654168

AIDA-2020

Advanced European Infrastructures for Detectors at Accelerators

Horizon 2020 Research Infrastructures project AIDA-2020

SCIENTIFIC/TECHNICAL NOTE

FIBRE TEST BENCHES FOR THE CHARACTERISATION OF MEDIA FOR CALORIMETERS WITH OPTICAL READOUT

Document identifier:	AIDA-2020-NOTE-2019-04
Note release date:	20/12/2018
Work package:	WP14 (JRA2): Infrastructure for advanced calorimeters
Lead beneficiary:	CERN
Authors	E. Auffray, M. Lucchini, P.Hobson, F. Cova, F. Moretti, K. Pauwels, A. Vedda, F. Nessi-TEDALDI, F. Micheli, G. Dissertori, S. Pigazzini, N. Bartosik, N. Pastrone,G. Tamulaitis, M. Korzik, V. Mechinsky, N. Akchurin, F. de Guio
Document status:	Final

Abstract:

For measurements of scintillating fibres, several test benches have been developed and commissioned within WP14 Task14.2.1, such as setups for attenuation length measurements, a test bench for the investigation of timing properties, and mechanical and data acquisition tools for studying the performance of scintillating fibres using high energy particles. The different setups are described in this document, providing additional details relevant for Milestone MS56 and Deliverable 14.1.

TABLE OF CONTENTS

1. INTRODUCTION

An essential part of the activities in WP14 is the development and construction of test infrastructures for calorimeter elements to support the R&D activities in the area of calorimetry for current and future collider detectors. Task 14.2 focuses on calorimeters with optical readout and is subdivided in two subtasks, subtask 14.2.1: *"Test benches for the characterisation of organic and inorganic scintillator fibres for future calorimetry"* and subtask 14.2.2: *"Test Benches for the Characterisation of highly granular Calorimeter Elements with Scintillator and SiPM Readout"*.

In the frame of sub task 14.2.1, several test setups have been developed for the characterisation and performance study of different types of fibres (heavy crystal fibres and light fibres based on SiO_2).

- Attenuation length measurement benches at CERN and at UNIMIB
- Uniformity measurement bench at ETHZ
- Pump and probe setup for timing properties investigation at Vilnius
- Test stand for the evaluation of light attenuation variation during irradiation at Brunel
- Co^{60} irradiation bench at CERN
- A setup to study SiO_2:Ce fibres as wavelength-shifters by ETHZ
- An absorber made of 0.75W/0.25Cu to evaluate the calorimetric performance of scintillating fibres (crystal and Ce and Pr doped SiO_2: fibres)
- A data acquisition system for high energy beam test setups

These different test benches provide an infrastructure for the in depth investigation of optical and radiation hardness properties of all types of scintillating fibres as well as their test in a calorimeter prototype.

In this note, we describe these different tests set-up, which have been commissioned over the last 4 years.

2. LIGHT ATTENUATION TEST BENCH @CERN

2.1. SETUP DESCRIPTION

In order to quantify the optical quality of the fibres and measure the propagation of the light along them, a setup to measure the light attenuation has been built at CERN. It is based on a double sided readout with two PMTs (see Fig.1). The sample to be measured is hold with two V-shaped mechanical supports. This makes sure to minimize the contact points when measuring the samples with no cladding/wrapping. Direct coupling with no optical coupling media (dry contact) is used as standard measurement since this minimizes the measurement error. The sample is excited with a light source of wavelength chosen to match one of the excitation bands of the scintillating material. The sample is generating isotropic luminescent light. Part of this light is propagating through the sample and reaching its ends, to be readout by the photodetectors. As opposed to a transmission/absorption measurement the attenuation measurement involves several modes of propagation of the light and assesses the light guiding properties of the fibres. Figure 1 shows the setup equipped with the LED pulser#2 designed by V. Mechinsky (RINP-BSU). This pulser comes with a 4 to 1 fan-in bundle of optical fibres and a collimator. This allows obtaining a very tiny spot of 2-3 mm to scan the fibre along its axis and to reduce the amount of parasitic light since the beam of light is shaped as a pencil. The output of the LED pulser is hold with a motorized stage and controlled with a computer. The signals of the two PMTs are digitized based on the SYNC OUT signal from the pulser (used as external trigger). The combination of a fast pulser (10-50 ns) with a high repetition (10-50 kHz) rate and a fast motorized stage allows making the measurement of a 20 cm long sample last for less than 30s.

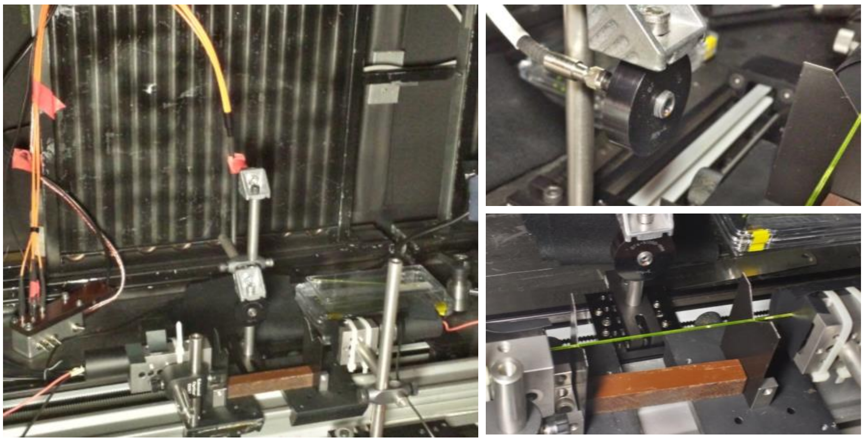

Fig. 1: *Setup for the measurement of the attenuation curves of the fibre-shaped samples equipped with a multi-wavelength LED pulser developed at CERN. The light is first coupled to optical fibres to bring the excitation light close to the samples with a collimator.*

To adapt for the various samples to be measured, several LED pulsers were built by RINP-BSU. A short history of the different version is presented here after (also see figure 2).

UV Pulser #1: prototyping

The first type of UV pulser was based on UV LED with emission maximum 365 nm. The pulser consists of two main blocs: a square-wave generator on the basis of NE555 timer and an electronic key (2N2222 transistor). The pulse duration was of 1500 ns with repetition rate of 13.5 kHz.

UV Pulser #2: Universal concept

This version uses more narrow pulses (50 ns) and a synchronized output (SYNC) to be used as external trigger in the DAQ system. Besides for more versatility, three output optical channels were integrated into the pulse: ~365 nm, ~400 nm and ~470 nm.

UV Pulser #3: Brighter and Faster

This version was dedicated to make the 365 nm LED brighter. A remote emitter is used here to avoid light losses through the optical fibre. An avalanche breakdown of a transistor in self-oscillation mode leads to a significant increase in response with an improved signal-to-noise ratio combined with a further decrease of the pulse duration (10 ns).

UV Pulser #4: 265 nm in addition to 365 nm

To be able to measure some samples with deeper UV excitation bands (e.g. Pr-doped fibres) a new pulser was built based on a UV LED with an emission peaking at 265 nm. To obtain sufficiently high operating voltages, a cascade of avalanche transistors powered with an external HV supply (+650 V) was chosen and for a more stable operation, the electronic key was modified to control the breakdown mode of the transistors. As in Pulser#3 the pulse duration is of 10 ns. This pulser is equipped with two remote probes (265 nm and 365 nm) for more versatility. Because of the increased operational voltage, the 365 nm LED is also brighter as compared to earlier pulsers.

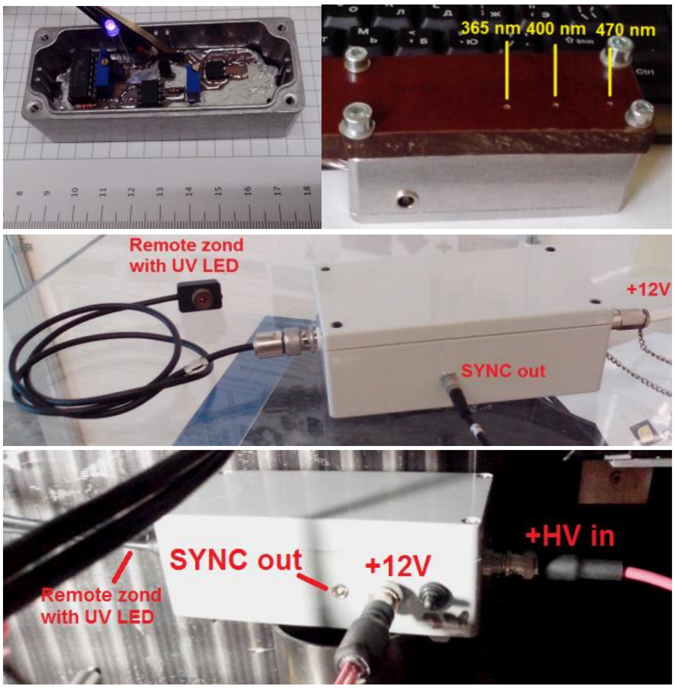

Fig. 2: *The four versions of LED pulsers produced by INP Minsk.*

2.2. EXAMPLE OF MEASUREMENTS

In Figure 3, some examples of recorded data set are shown for a high quality Czochralski grown crystal fibre of YAG:Ce and a sample of poor optical quality for which the good dynamic range of the setup is valuable.

The detection of the luminescent light at both ends of the fibres is very useful to mitigate alignment problems and minimize the influence of scattering centers on the excitation light. By computing the ratio of both signals, these fluctuations in the intensity of the excitation light are cancelled out.

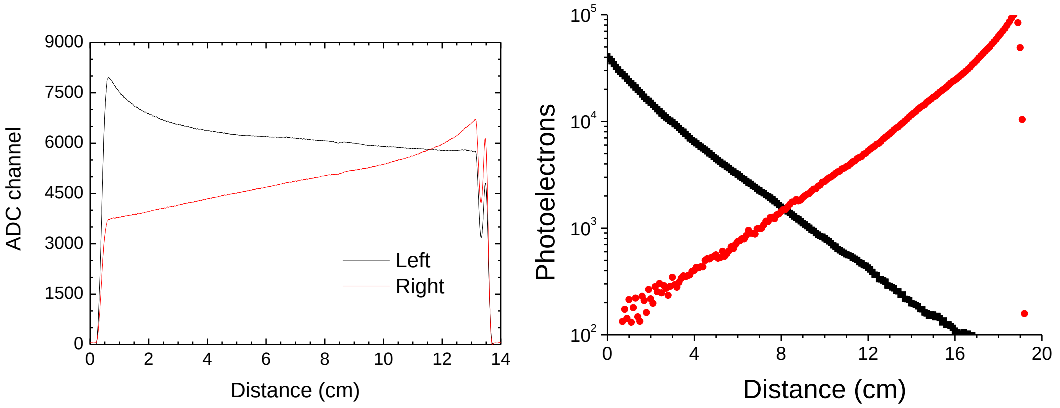

Fig. 3: *Example of attenuation curves acquired on high quality fibres (left) and on fibres of poor optical quality (right). From the left plot, we can estimate the spatial resolution of the setup which is very good as can be seen from the sharp peak at d=13.5 cm due to the V-shaped masks. On the right plot, the good dynamic range of the setup is illustrated, ranging from a few tens of photons up to 100'000 photons.*

In figure 4, the attenuation length measured on Ce doped silica fibres before and after irradiation are presented.

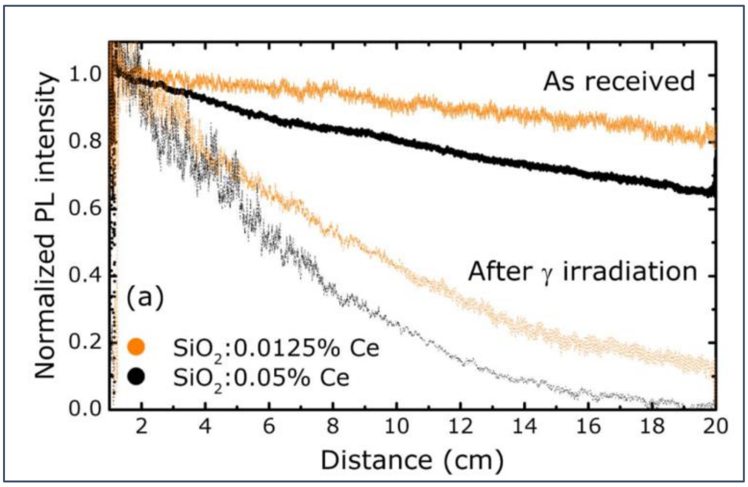

Fig. 4*: Attenuation length curves for SiO_2:0.0125% Ce- and SiO2:0.05% Ce-doped fibres before (solid lines) and after (dotted lines) 1 kGy γ irradiation.*

2.3. CONCLUSION

This set-up is operational to perform characterisation of the light attenuation of various types of scintillating fibres. It has been largely used in the last years.

3. OPTICAL ABSORPTION MEASUREMENT SYSTEM @UNIMIB

3.1. SETUP DESCRIPTION

In order to measure the optical absorption of (scintillating) optical fibres, UNIMIB developed a system, which is composed by a Perkin Elmer Lambda 950 double beam spectrometer equipped with an accessory (see Fig.5), which is able to inject and collect light into, and from, suitably designed optical fibres. The spectrometer is by itself able to cover the entire spectral range from 190 to 3300 nm (from UV to near infrared) with a maximum photometric range of the order of 6 absorbances.

The accessory for fibre measurements is composed by two curved mirrors and two lenses to focus the light beam on the fibre core and match the numerical aperture of the fibres with that of the instrument. The measurable fibres length can vary in a range of few centimetres up to a couple of meters; it is also possible to measure various fibre shape and diameter. According to Perkin Elmer and to our own experience, the accessory has a throughput of the order of 10 % when using 600 µm core fibres.

In order to reliably couple the accessory with the fibres under test, two "launch" fibres have been prepared from a commercial fibre (Polymicro FDP 600, high OH silica, core 600 mm, numerical aperture 0.22). Due to the transparency characteristics of the two launch fibres, the usable range of the spectrophotometer is reduced to about 190-1200 nm. These two fibres have SMA connectors on one end (as an interface with the instrument) and FC connectors on the other (to be connected to the to-be-measured fibre). The choice of the FC connector to join the launch fibres to the tested one is motivated by the higher reliability and reproducibility of this kind of connectors with respect to others. This however implies that the fibres under test must be terminated with FC connectors. A further extension of the current set-up has been designed to make the system more versatile and able to measure reliably fibres without connectors. It makes use of two translating lens mounts with micrometric precision equipped with FC/PC fibre adapter plates with external SM1 thread, in order to hold the fibres without any other support, and to connect each fibre end with one out of the two "launch" fibre. The distance between the two mounts can be adjusted by installing them on a rail, to allow measurements of fibres of various lengths, ranging from few centimetres up to some tens of centimetres.

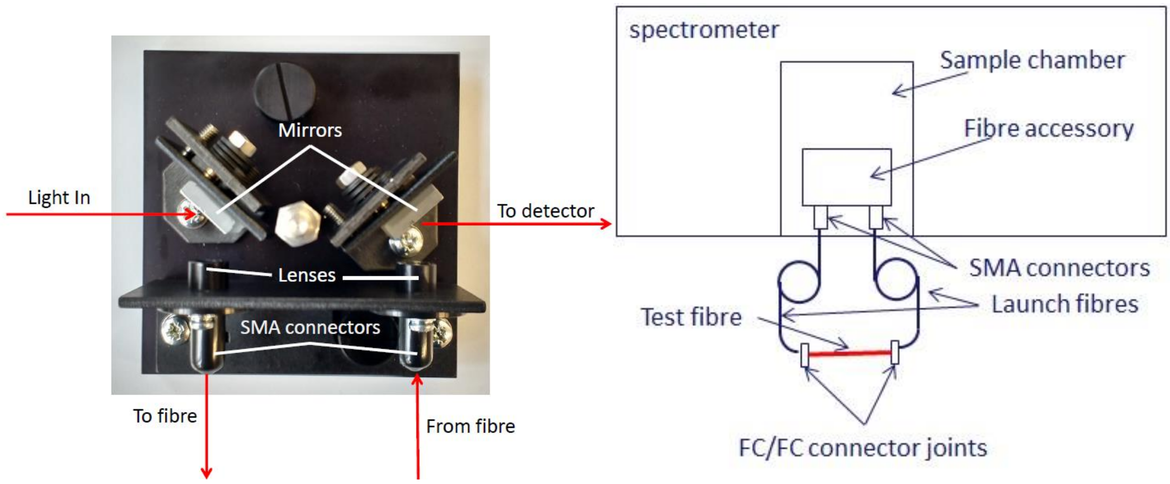

***Fig. 5.:** Left panel, picture of the Perkin Elmer accessory for optical absorption measurements on optical fibres. Red arrows, optical path. Top cover removed. Right panel, scheme of the complete spectrophotometer system.*

3.2. EXAMPLE OF OPTICAL ABSORPTION (OA) MEASUREMENTS ON SiO_2:CE SCINTILLATING OPTICAL FIBRES

The setup for the optical absorption measurements of fibres has been extensively employed to characterise the radiation resistance of Ce or Pr -doped silica fibres with different concentrations of dopants, as reported in [1, 2]. As an example of the kind of results that can be obtained with the instrument, figure 6 presents two measurements performed on scintillating Ce doped silica fibre (core diameter 600 µm, F-doped silica cladding 750 µm, Ce concentration 500 ppm) before and after irradiation with ^{60}Co γ-rays.

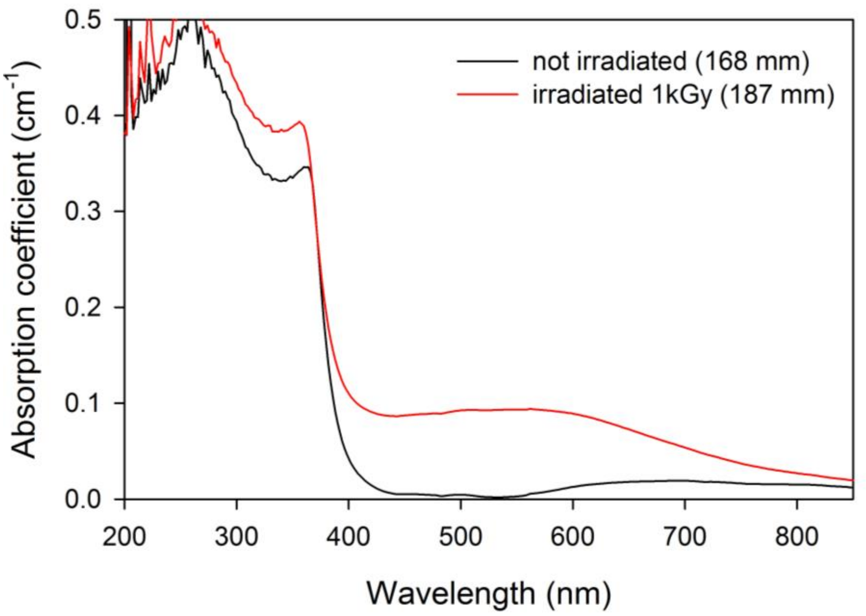

Fig. 6: *Optical absorption spectra of SiO_2:500 ppm Ce optical fibre before and after irradiation with 1 kGy ^{60}Co γ-rays*

The spectrum of the not irradiated sample shows complex structures below 400 nm likely related to Ce^{3+} 4f - 5d transition and charge transfer of Ce^{4+}. The region below 400 nm is also distorted by Ce^{3+} luminescence. The broad and weak absorption structure visible in the not irradiated sample above 600 nm is probably related to intrinsic defects. After irradiation, the picture is modified by the presence of further well evident absorption contributions in the blue-green region of the spectrum related to the formation of colour centres induced by irradiation; these new, radiation-induced absorptions strongly overlap with the emission spectrum of Ce^{3+} (which is centred at about 450 nm). The spectral information of light attenuation allows, then, an evaluation of the radiation-induced band impact on the luminescence characteristics of the fibres in terms of absolute absorbed light and of spectral modifications of the transmitted light.

3.3. CONCLUSION

The optical absorption set-up for measuring optical fibres is currently working, and it is being regularly used to characterize scintillating rare earth doped SiO_2 fibres. The system is of simple and rather quick use; it also has high sensitivity and reproducibility. The obtained information is very valuable since it contains also the spectral composition of the absorbing species: this is particularly interesting in the evaluation of scintillating fibre radiation hardness. However, in the case of luminescent fibres the obtained spectra can be distorted by luminescence contributions, and attention must be paid in spectra analysis and interpretation. The luminescence issue can be resolved by considering also the use of appropriate filters.

4. UNIFORMITY TEST BENCH @ETHZ

4.1. SETUP DESCRIPTION

A laboratory test bench has been set up and commissioned for the measurement of the signal uniformity of scintillating fibres along their length (Fig. 7). The bench has been commissioned by measuring the light uniformity response of scintillating fibres with and without aluminisation at the end opposite to the photodetector. A Sr ^{90} source is used for the excitation of the fibres. Measurements show (Fig. 8) that, while uniformity is only slightly affected and remains within the 5% of the measurement accuracy, the aluminisation allows to collect 25% more signal.

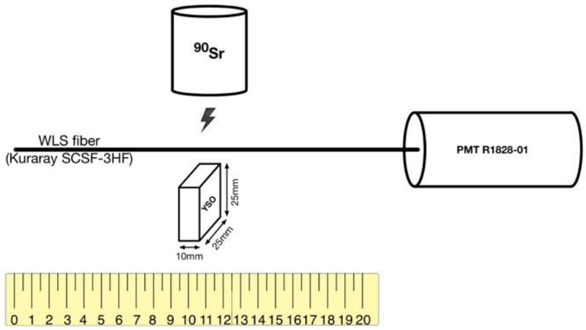

Fig. 7: *Schematics of the laboratory setup developed for fibre uniformity measurements*

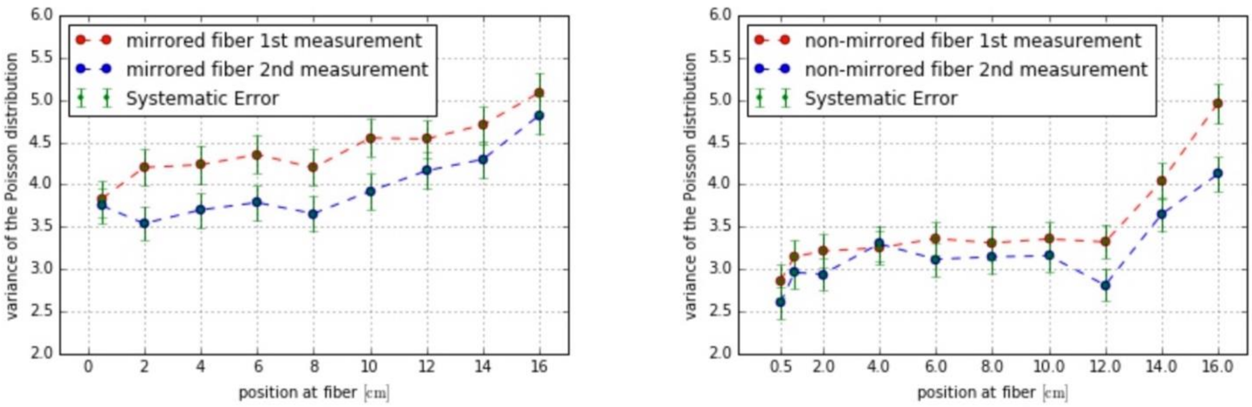

Fig. 8: *Signal amplitude versus source position along a fibre with (left) and without (right) aluminisation.*

5. PUMP AND PROBE TEST BENCH @VILNIUS

5.1. SETUP DESCRIPTION

The test bench for pump and probe study (TBPP) is dedicated to monitor dynamics of i) two–photon absorption, ii) population of photo-excited states, and iii) free carrier absorption in scintillation materials. The main configuration of TBPP is presented in Fig. 9, while the general view of the set-up is shown in Fig. 10.

For free carrier absorption experiments, a KGW:Yb laser generating 200 fs pulses and equipped with harmonic generators and a parametric amplifier to ensure tunability of the pump photon energy was exploited as a pump source. The samples are probed by a white light continuum in the range from 1.3 to 2.7 eV generated in sapphire using a part of the laser radiation. The variable optomechanical delay of the probe pulse in respect to the pump pulse enabled measurements of time evolution of the transient absorption with time resolution limited only by laser pulse duration. The difference in the optical absorption with and without the pump (differential absorption, DA) is measured as a function of the delay between pump and probe pulses. The DA is caused by the induced absorption, which is proportional to the density of nonequlibrium carriers: the electrons in the conduction band, the holes in the valence band, the carriers located at activator ions and trapped at defect-related levels. The contributions of the different populations are revealed by their spectral signatures under selective excitation of different structural units of the crystal.

For two photon absorption experiments, a monochromatic probe beam is exploited. The wavelength of the probe beam is tuned by using harmonics generators and an optical parametric amplifier "Orpheus" providing 200 fs pulses continuously tunable in the range 630–2600 nm (the range can be extended down to 315 nm by frequency doubling).

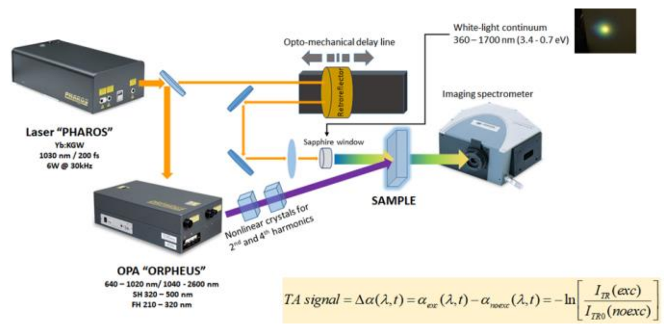

Fig. 9.: *Schematic outline of pump and probe configurations*

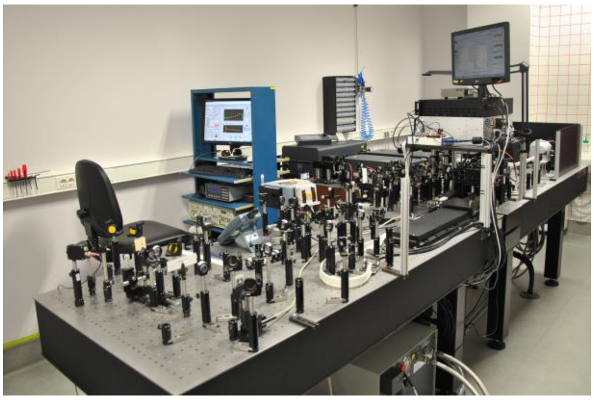

Fig. 10: *Test bench for pump and probe study*

The figure 11 presents an exemple of transient absorption spectra versus probe delay and probe photon energy obtained with the set-up.

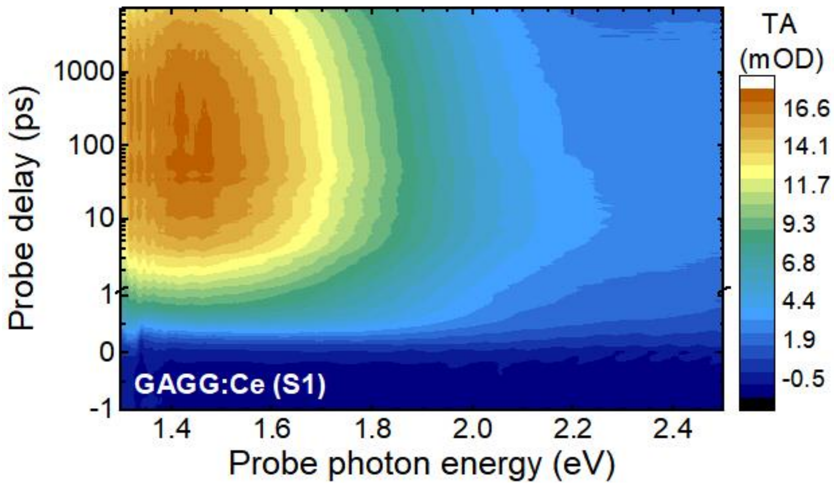

Fig. 11*: Example of a transient absorption spectra*

This setup has been used to characterised several scintillating materials see [3,4,5,6,7,8].

6. TEST STAND FOR EVALUATION OF LIGHT ATTENUATION VARIATION DURING IRRADIATION @ BRUNEL.

A fibre test stand to enable the determination of real-time degradation of absorbance in optically transparent fibres during irradiation has been designed and is being commissioned at Brunel University London. Real-time measurement of what could be fairly short-lived colour centres is potentially important for an understanding of issues relating to particular scintillating or wave-length fibres that are considered for use in new designs of calorimeters with optical readout.

6.1. DESIGN PARAMETERS

To evaluate changes in optical absorbance and, in principle, fluorescent yield of a WLS fibre, we have designed a test stand that will be used remotely from the light source and spectrometer as the radiation is produced by a Co^{60} source which will rapidly damage any electronic systems within the cell. Due to the chicanes in the shielding we need to be located at least 20 m from the radioactive source during an exposure. For these reasons we have designed a system using a fibre-coupled light source and a fibre-coupled UV-visible spectrometer. These instruments are then connected by 20 m lengths of pure-silica core step-index fibres to the test stand itself (see Fig.12), [9].

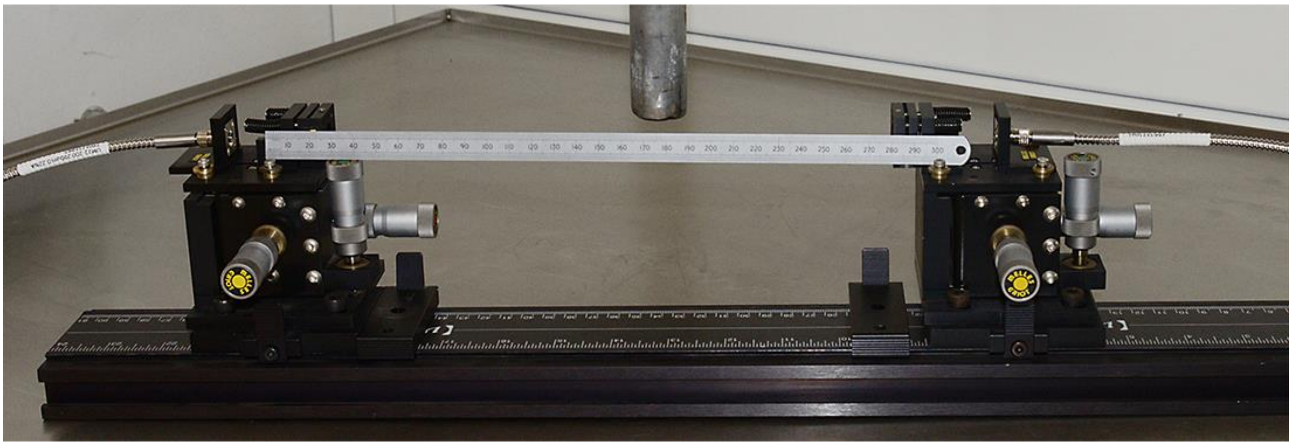

Fig. 12*: Fibre test bench. The two optical fibres, connecting the remote spectrometer and light source respectively, come from left and right and light is focussed onto the fibre under test by silica lenses located within the precision manual x-y-z stages. The Co^{60} radioactive source, when exposed, is located at the bottom of the steel tube seen in the centre of this photograph. The fibre under test is placed in a holder (not shown) located in the gap between the stages.*

The key components used in the test bench are listed in the table below:

Component	**Model/Description**	**Characteristics**
Spectrometer	StellarNet Black Comet spectrometer BLK-C 100	Wavelength range: 190 nm – 850 nm Detector: CCD with 16-bit ADC. Maximum integration time is 65535 ms.
Light Source	StellarNet SL5	Combined Deuterium & Tungsten Halogen light source.
Fibres	Two 20 m lengths of Thorlabs UM22-200	0.22 NA, 200 μm diameter silica core, step-index fibre.
Focusing lenses	Two Thorlabs LB4003	UV silica biconvex lens uncoated, 12.7 mm diameter, f = 30 mm.

6.2. SPECTROMETER PERFORMANCE

The spectrometer has been fully characterised, the following bullet points summarise the main conclusions:

- Sequentially captured spectra show a very similar mean signal level to within a few counts averaging across the full spectral histogram;
- The dark current signal level is low (~ 200 counts mean for 180 ms integration time) compared to the peak of a measured light source spectra (see Figure 10), a variation of 100 counts in dark signal being a fluctuation of around 0.25% of the peak counts (~42000) in a collected deuterium, halogen light source combined spectrum;
- Data collected at different integration times shows that readout amplifier noise dominates the resulting spectrum until the integration time is increased beyond 2000 ms. Increasing the integration time further results in an approximately linear increase in observed dark current with increasing integration time.

Figure 13 shows the recorded spectra of the deuterium-halogen light source after 20 m of optical fibre. No correction for the wavelength dependence of the fibre absorption or the variation in response with wavelength of the CCD detector in the spectrometer has been applied.

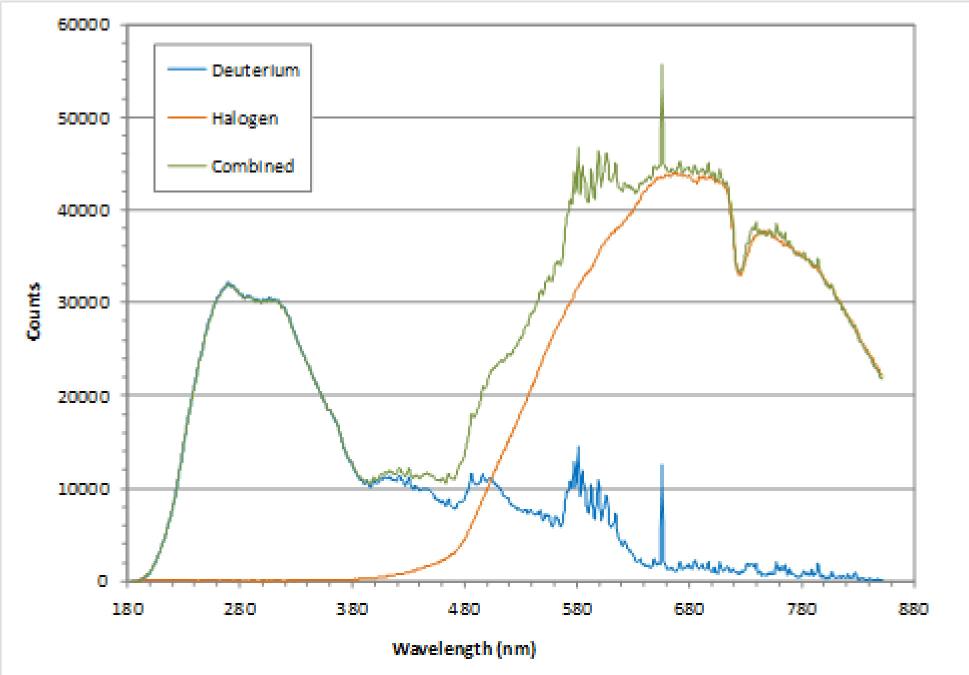

Fig. 13:. Recorded spectra with spectrometer connected with one length of 20 m fibre directly to the deuterium/halogen light source. The spectra are uncorrected for any variation in CCD response with wavelength and the integration time was 180 ms. The "combined" curve is taken with both light sources on simultaneously.

6.3. OPTICAL SYSTEM CHARACTERISATION

Figures 14 and 15 show the predicted sensitivity of the optical system to misalignment of the fibre under test. Optical modelling was done in ZEMAX OpticStudio in non-sequential mode and the fibre under test was assumed to be a 100 mm long, 2 mm diameter quartz rod with no cladding and planar faces. Such a reference fibre has recently been ordered from UQG Optics Ltd, Cambridge.

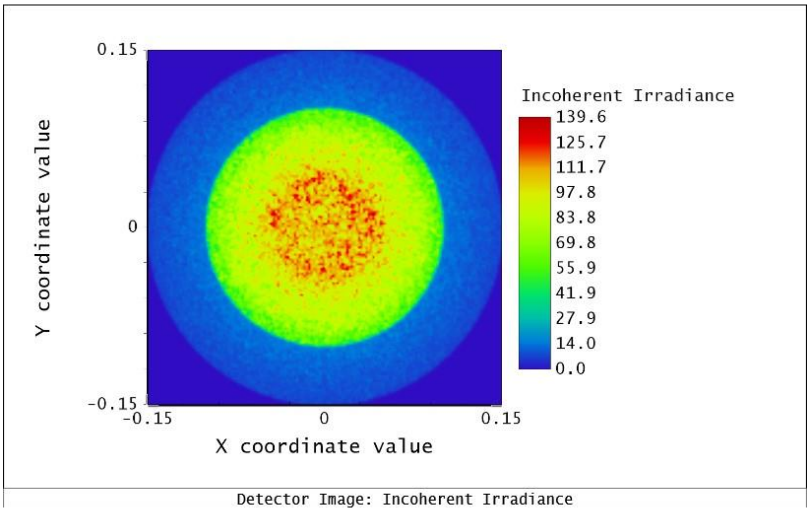

Fig. 14: *The incoherent irradiance in the optical fibre taking light back to the spectrometer following the collection lens. The light has traversed a perfectly aligned quartz rod of 2 mm diameter. The core diameter of the collection fibre was 200 µm*

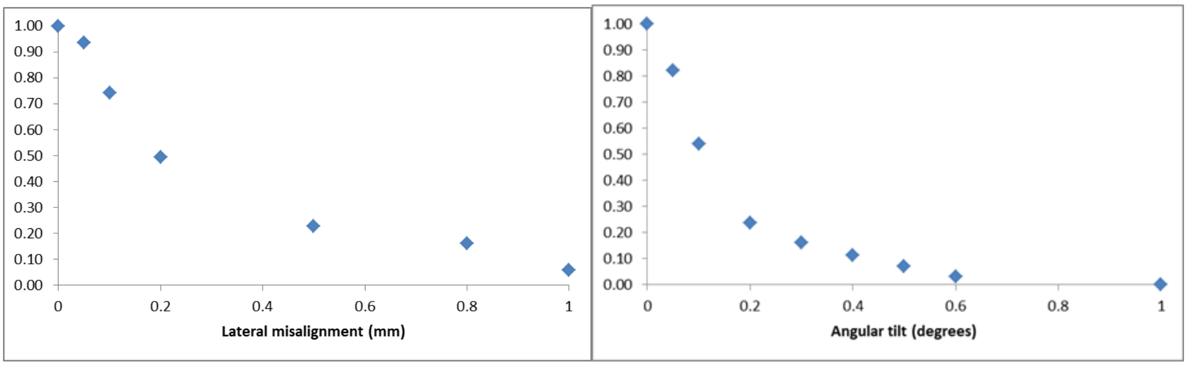

Fig. 15: *Predicted effects, using ZEMAX OpticStudio software, of lateral and angular misalignment of a 100 mm long, 2 mm diameter quartz rod in the fibre test bench. Both curves illustrate the decrease in optical power coupled from the rod into the fibre returning from the test bench to the spectrometer. The data are normalised to the value of the coupled power for perfect alignment.*

6.4. IRRADIATION RESULTS

To test our system we irradiated a 3 mm diameter. 150 mm long rod of PMMA (standard commercial PMMA with UV inhibitor) continuously in our Co^{60} facility to a total dose of 10 kGy over a period of four days. Measurements were taken during the period with the spectrometer always on and the combined tungsten/deuterium fibre-coupled light source on only when measurements were taken, allowing a five minutes warm up before data recording. Figure 16 shows the change in transmission, after dark current subtraction, in the region near the UV cut-off where the largest effect of radiation induced damage was seen.

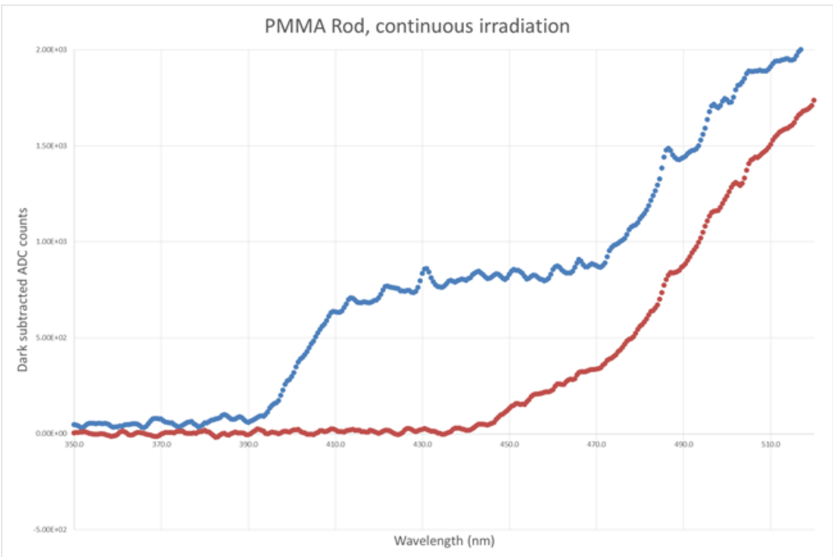

Fig 16: *A 3 mm diameter rod, 150 mm long of standard PMMA (with a UV cut-off around 395 nm) was irradiated in the dark for 4 days to a total absorbed dose of ~ 10 kGy. Top curve (blue) shows the transmission before irradiation, the lower (red) curves show the transmission after 10 kGy dose. A combined deuterium and W-halogen light source was used to measure transmission. An average of eight, 8 s exposures was used for both the signal and dark current.*

During this test we discovered that removing the 20 m long fibres to the sample under irradiation and directly coupling the light source to the spectrometer for a calibration run before each sample measurement introduced significant variations due to a lack of precision in the spectrometer fibre connector. We are currently evaluating the repeatability of the light sources during a long data taking period when periodically power cycled.

7. CO^{60} IRRADIATION BENCH @ CERN

In order to study the radiation hardness of the samples, a secured Co^{60} source of high activity (2.5 GBq) is available at the CERN group laboratory (see Fig. 17). Samples can be exposed to the gamma rays at a rate of ~1 Gy/day.

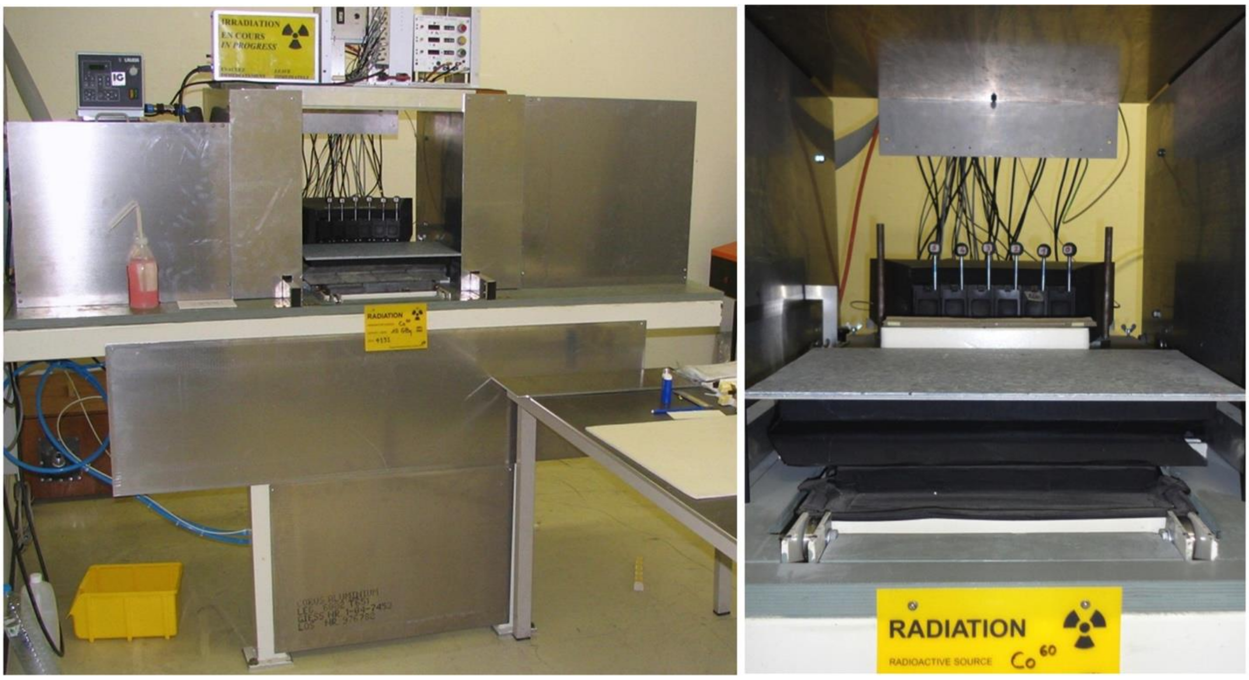

Fig.17: *Pictures of the Co60 radioactive source used for studies on radiation hardness.*

Access to Co^{60} source allowing higher dose rate (500Gy/h) near CERN is also available for Aida project as well as the PS proton irradiation facility, IRRAD, at CERN. These irradiation facilities allow evaluating the radiation behaviour of the investigated materials at the radiation level required in future high energy experiments.

8. A DATA ACQUISITION SYSTEM FOR HIGH ENERGY BEAM TESTS

A data acquisition for high-energy beam test setups has been developed, commissioned and maintained under the responsibility of two postdoctoral researchers (F. Micheli and S. Pigazzini, ETHZ), where the former was hired through AIDA for this purpose. It has been used for the tests performed since 2015 in the H4 beam line at the CERN SPS accelerator [10].

The core system has been built around the ZeroMQ library, which provides a low latency communication over ordinary networks, allowing to operate several instances of the DAQ on different machines. A typical configuration used during the tests described in this report included a master application interfaced to the SPS communication system and a slave instance, running on a PC close to the setup, which reads out the data from the detectors. Although the DAQ system is built with a general API that can be interfaced to different hardware, throughout the beam tests we extensively used the CAEN V1742 VME board. The V1742 includes 4 DRS4 chips that allows sampling the detector signal at frequency up to 5 GHz for a total of 32 channels capable of providing detailed sampling of pulse shapes and excellent time resolution. The choice of this flexible configuration enabled us to optimize the signal reconstruction offline.

The DAQ system also allows to read out and reconstruct the information provided by the wire chambers and hodoscopes positioned in the beam line and thus to associate the particle impact point to each event. The software is also configurable to read out the information from a multi-channel ADC. The DAQ system is synchronized with the beam signal provided by the syncrotron facility (e.g. PS or SPS) and requires a trigger which can be provided by standard scintillators.

The software also includes tools for data quality monitoring (DQM) which produce a quick analysis of the data to monitor the beam intensity, position, etc. and a user interface GUI to control both the DAQ and DQM.

All software has been released on github and can be downloaded and reproduced on multiple machines with small changes in configuration files:

https://github.com/cmsromadaq/H4DAQ

https://github.com/cmsromadaq/H4DQM

https://github.com/cmsromadaq/H4GUI

The main beam test studies which have been performed with this DAQ system include:

- Timing resolution measurements of Lead Tungstate scintillators amnd LYSO in collaboration with CMs -ECAlcollaboration
- W/CeF_3 sampling calorimeter with Ce doped quartz fibres as WLS
- W/LYSO Shashlik calorimeter with capillaries
- SPACAL calorimeter with heavy scintillating fibres

9. A SETUP TO STUDY SIO_2:CE FIBRE AS WAVELENGTH-SHIFTERS @ ETHZ

9.1. DESCRIPTION OF THE FIRST SETUP

A test setup has been developed in order to study SiO_2:Ce fibres as wavelength-shifters in a sampling calorimeter single-channel prototype that uses CeF_3 as a scintillator (Fig.18). The readout system developed and commissioned in 2015 (see section 8) has been used for that purpose at the CERN SPS accelerator. The test has allowed to observe that SiO_2:Ce fibres exhibit, as visible in Fig19, the following properties:

- the WLS emission time constant typical of Cerium (folded in twice in this setup)
- a fast Cherenkov component (rise time few ns, dominated by PMT response time).

The observed response could be exploited in timing measurements, and for this purpose, dedicated tests have been performed.

Fig. 18: *W-CeF$_3$ calorimeter channel, during assembly*

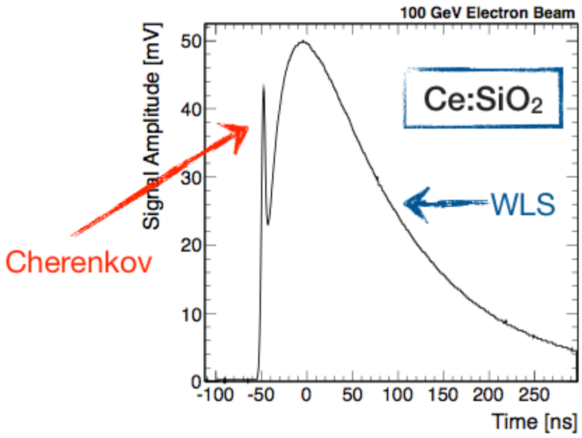

Fig. 19: *W-CeF$_3$ calorimeter signal, exhibiting the slower, wavelength-shifted scintillation time constant, and a fast Cherenkov component*

The Cherenkov component of SiO_2:Ce fibres has been studied in a dedicated test. For this test, Hamamatsu SiPMs have been used, read out by a preamplifier board developed by ETH for this purpose.

The direct Cherenkov light from SiO_2:Ce fibres has been detected by blinding one bundle towards the Cerium Fluoride scintillation light (Fig.19, left). The timing resolution constant term achievable for electrons impacting on the fibres is below 100 ps (Fig. 19, right). The calorimeter remains as an infrastructure for tests of various fibres.

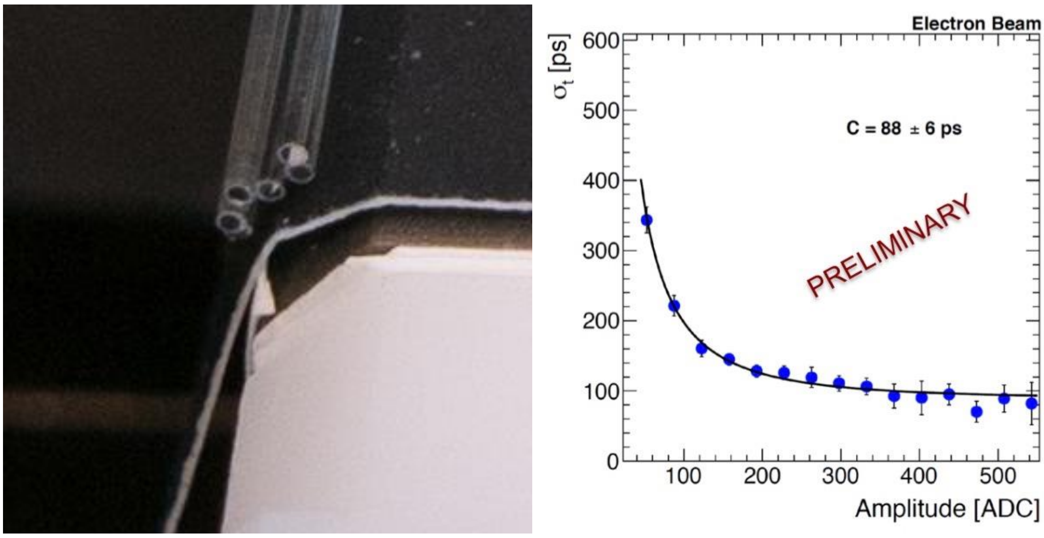

Fig. 20 Left: *SiO_2;Ce bundle screened by black paper from receiving the calorimeter scintillation light*
Right*: Timing resolution for the W-CeF_3 calorimeter, read out by SiO_2:Ce WLS fibres, as a function of signal amplitude.*

A matrix of 5 x 3 channels (Fig.21) has been prepared and tested in beam in June 2016 at CERN. Construction parameters were:

- Dimensions: 12 x (6mm CeF_3 + 5 mm W) x 25X0, transverse dimension 17 mm (Fig. 20, right)
- High granularity: R_M = 17 mm
- WLS fibres for readout: Kuraray 3HF-SC, 1 mm diameter
- 3 mm-wide, depolished chamfers to favour scintillation light escape towards the WLS fibres, thus dimensioned to accommodate fibres
- 4 fibres signals onto one photodetector, read out independently for one single channel (in green in Fig. (20, left)
- APD readout, as for the CMS ECAL barrel

Fig. 21. Left*: Layout of the W-CeF3 matrix.* ***Right****: Photograph of one matrix channel during assembly.*

9.2. DESCRIPTION OF THE SECOND SETUP

In June-July 2018, several new types of Ce-doped fused-silica fibres have been studied using high energy electrons by ETHZ group in collaboration with Texas Tech. The main objectives were to establish or confirm:

- The scintillation (radioluminescence) light yield and pulse shape of (irradiated/un-irradiated) fibres when exposed to charged particles, and

- The wavelength shifting (photoluminescence) efficiency of (irradiated/unirradiated) fibres when coupled to a CeF_3 crystal.

The setup for fibre characterisation in the high-energy electron beam is shown in Fig. 22, left, while their wavelength-shifting characteristics have been studied by coupling them over an air gap to a CeF_3 crystal (Fig. 22, right).

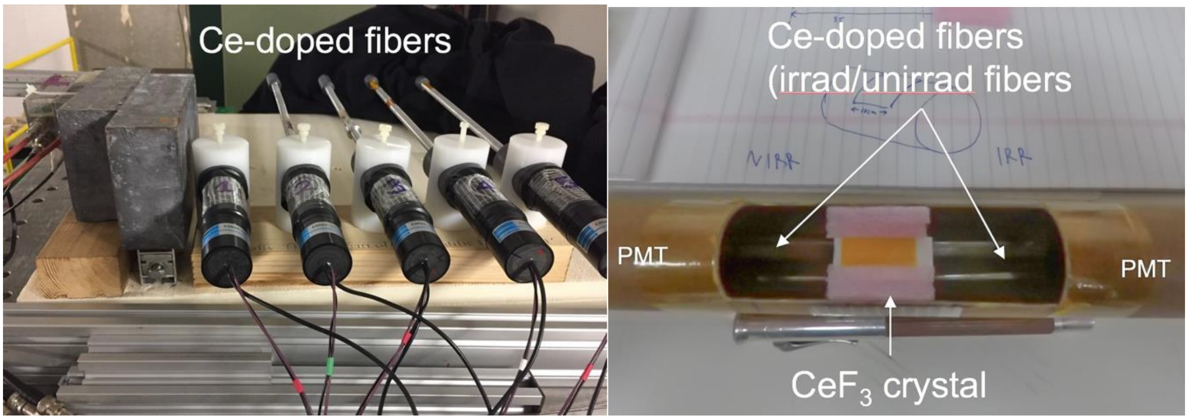

Fig. 21: *Test beam setup for the characterisation of Cerium-doped fused-silica fibres (left) and setup with two fibres coupled to a CeF_3 crystal for their evaluation as wavelength-shifters (right).*

Fibres were compared, of Phase-2 (Fig. 23, left) and Phase-4 (Fig. 23, right), the latter one before and after having been irradiated, to extend studies described in [11].

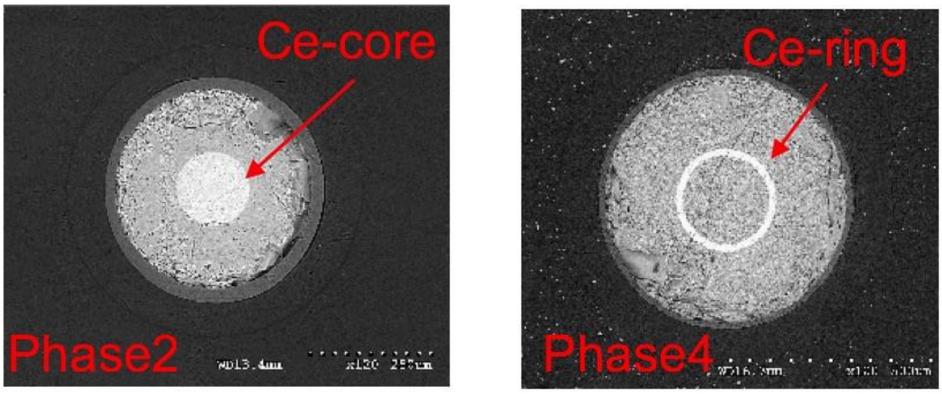

Fig. 23: *Phase-2 (left) and Phase-4 (right) fibre structure, where the distribution of photoluminescent cerium is in the core and in a ring around the core, respectively.*

Some preliminary results are visible in Fig. 24. Final analysis for a journal publication is in progress.

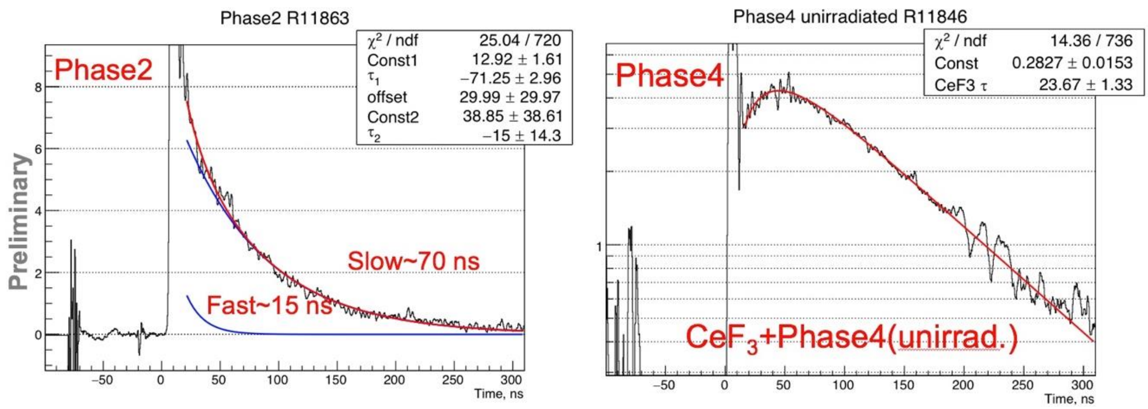

Fig. 24: *Pulse shape of the Phase-2 fibre signal (left) and pulse shape of the wavelength-shifted Phase-4 fibre signal originating due to cerium fluoride scintillation (right).*

10. AN ABSORBER MADE OF 0.75W/0.25CU TO EVALUATE THE CALORIMETRIC PERFORMANCE OF SCINTILLATING FIBRES

In order to evaluate the energy resolution of a fibre based calorimeter in high energy particle beams, a dedicated prototype has been built in a configuration where the fibres are pointing to the beam, commonly referred to as SPACAL.

10.1. DESCRIPTION OF SETUP

The setup is composed of an absorber made of 40 plates of 0.75W/0.25Cu with grooves of 1.1x1.1mm^2, 1.8 mm apart (see Fig 25). The plates are stacked together and fixed by two stainless steel plates at the top and bottom of the module. The absorber contains a total of 1200 holes and has an overall dimension of 60x60x200mm^3. The dimension has been defined in order to achieve full energy containment of electromagnetic showers with energy up to ~200 GeV for scintillating and/or Cerenkov fibres of density between 2.7 and 7.3 g/cm^3.

The light produced by a group of 11x11 fibres is readout simultaneously with a photodetector (PMT or SiPM) optically coupled to the end of fibres through an optical light guide in order to increase the light collection and reduce the channel counts (See Fig. 26). The module consists thus of a 3x3 channel array, where each channel is about the width of one Moliere radius and contains 80-90 of the shower. If needed the read-out granularity can be increased by developing a new system of light guides and by increasing the number of photodetectors.

The fibres can be easily inserted and removed from the module without the need to disassemble the tungsten-copper plates and thus testing of different types of fibres in relative short time is possible.

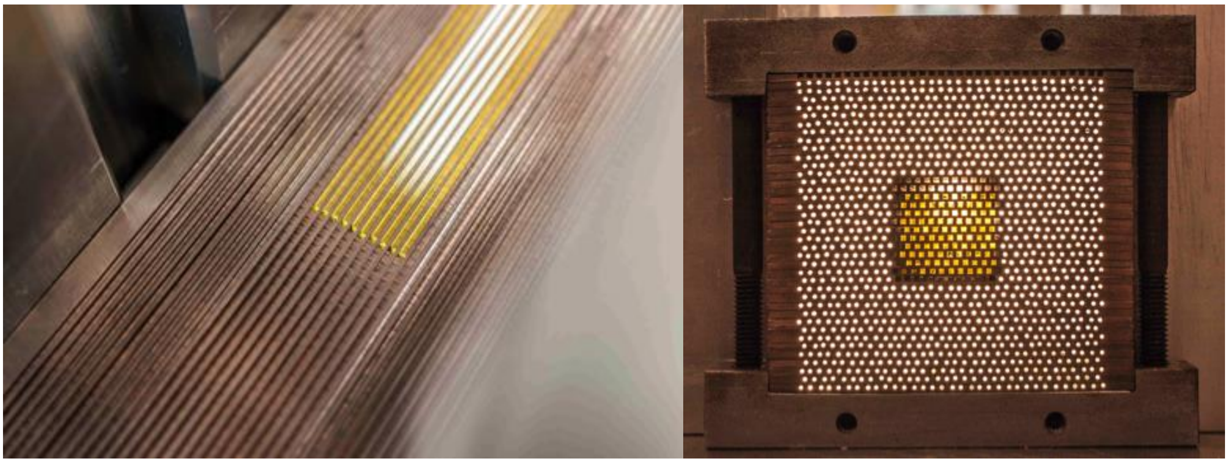

Fig. 25: ***Left****: Plate of 0.75W/0.25Cu with groove to insert the fibres,* ***Right****: completed absorber made of X plates*

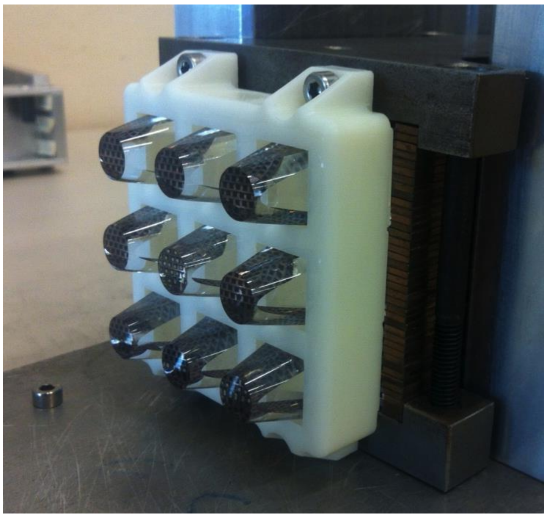

Fig. 26: *Light guide at the end of the fibres*

10.2. COMMISSIONING OF THE SETUP

The prototype made of the Tungsten-Copper absorber has been demonstrated to be valid with 121 fibres of YAG fibres crystals in the central channel and 1500 plastic fibres to fill the remaining fraction of the absorber. The 9 channels have been read-out with individual PMTs and signals produced by electron showers between 50 and 200 GeV have been measured. The energy distributions are reported in Fig.26. This first beam test allowed commissioning the module layout and its read-out by measuring the response of both plastic and crystal fibres whose signal was digitized with a CAEN V1742 digitizer.

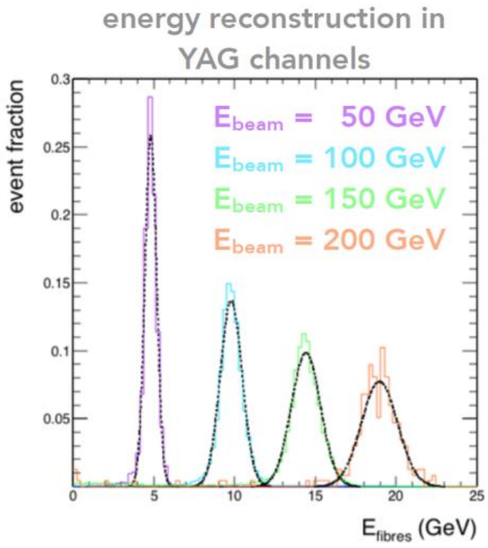

Fig. 27: *Energy reconstruction in YAG fibres*

10.3. TEST WITH SPACAL ABSORBER

10.3.1. Test of ce-doped sio_2 fibres with SPACAL absorber

The tungsten-copper absorber described in the previous section has been employed to investigate the scintillating response of Ce-doped silica fibres under exposure to electrons in the 20 – 200 GeV energy range, in order to explore the feasibility of silica-based fibres for a simultaneous dual Cherenkov and scintillation readout approach [12] during a test beam campaign in H4 beam line of the CERN SPS North Area facility in 2017.

The previous setup has been adapted to measure five distinct channels of fibres, sketched in Fig. 28c, filled with 80 fibres each for a total bundle diameter of approximately 15 mm: fibres were YAG:Ce (central channel), 0.002% Ce-doped silica (top left), plastic Kuraray SCSF-3HF used as reference (top right), 0.05% and 0.0125% Ce-doped silica (bottom left and right respectively). A smaller absorber block, shown in Fig. 28 (b) was also filled with 50 Pr-doped silica fibres.

A set of 6 Hamamatsu Photonics R5380 photomultiplier tubes (PMT) with bialkali photocathodes and borosilicate glass windows of 20 mm diameter were used to read out the light from the fibres in the SPACAL module: top channels were read out only from the rear side, bottom channels from both sides of the fibres, to exploit the use and the advantages of the double side readout technique. Pr-doped fibres in the mini- SPACAL prototype were read out from both sides with two UV-sensitive Hamamatsu H6610 PMTs with quartz windows, operated at 1000 V. Silicon rubber optical interface (EJ-560, Eljen Technology) with refractive index of 1.43 was used to couple the fibres and the PMT window, in order to improve light extraction.

The module was mounted inside a light tight aluminium box providing optical and thermal insulation, with a water cooled system to maintain a constant temperature of 18 ± 0.5 °C: the box was installed on a remotely-controlled horizontal - vertical (x - y) table with a displacement range of ± 300 mm and positioning accuracy of about 1 mm.

The module was exposed to the beam both in pointing and transverse configurations, described in Fig. 28 (d). In the former case, the beam was aligned with the fibres and the shower of secondaries developed all along the fibres length, while laterally extending inside the fibre bundle; the Moliere radius was in fact estimated to be around 17 mm. In this configuration, the analysis of the time decay of the emitted light intensity and the study of the fibres response as a function of varying incident beam energy were performed. In the transverse configuration, the analysis of the attenuation profiles through a position scan in steps of 30 mm was carried out.

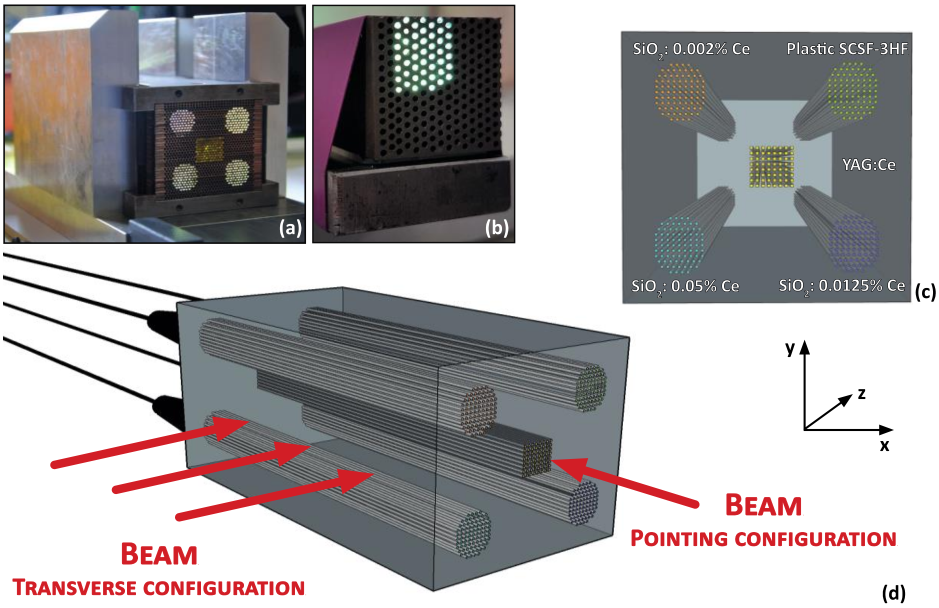

Fig. 28: *SPACAL setup. (a) Picture of the SPACAL prototype made of 5 channels with 80 fibres each in a tungsten-copper absorber; (b) picture of the mini- SPACAL with 50 Pr-doped silica fibres in a tungsten-copper absorber. (c) Schematics front view of the SPACAL prototype: the labels describe the type of fibres in each channel. (d) Schematics side view of the SPACAL module, showing pointing and transverse configurations.*

The SPACAL prototype was proven to be a valid tool for the evaluation of the scintillation and calorimetric performances of silica fibres under high energy electrons probe: time-resolved spectroscopy (Fig. 29 left panel), attenuation length profiles both in transverse (Fig. 29 right panel) and pointing configurations, and the reconstruction of the energy distributions were addressed. A discrimination method to well distinguish Cherenkov and scintillation emission contributions was also developed.

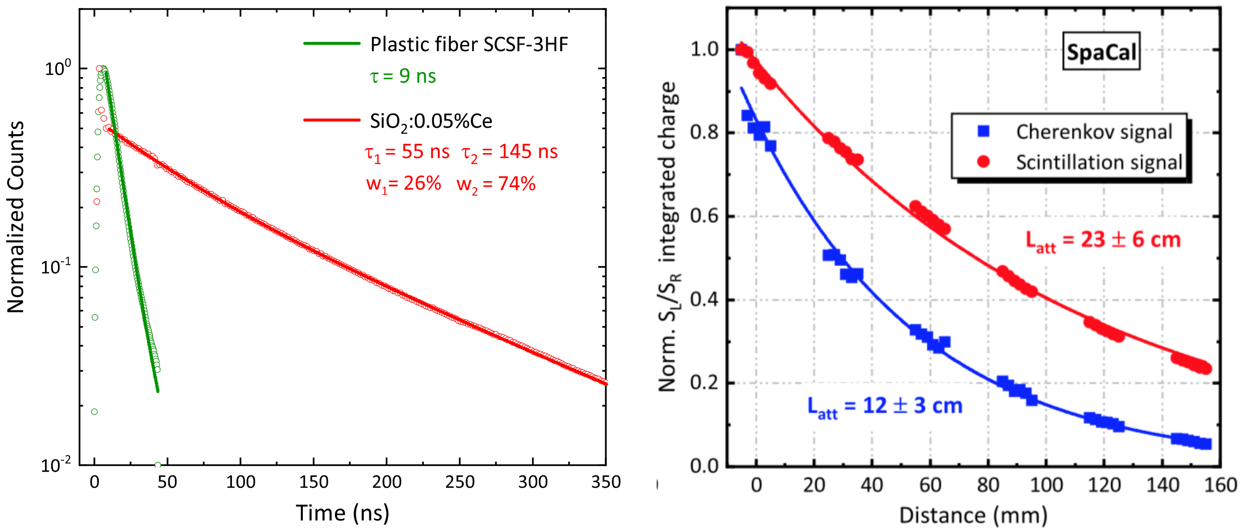

Fig. 29: *Left: normalized average pulse shape of Ce- doped silica and plastic fibres (dotted lines) and fit of the scintillation decay (solid lines) with a sum of exponential contributions for 150 GeV electrons beam. In the legend, decay time and weight of each component are reported. Right: Attenuation length curves for SiO2:Ce doped fibres measured in transverse configuration under 150 GeV electrons beam and using the double readout technique: on the y-axis, the ratio of left over right PMT signal is reported. Discrimination between Cherenkov and scintillation signal is considered.*

10.3.2. Test of ce-doped sio$_2$ fibres with spacal absorber with SIPM array

In order to investigate the potential of SPACAL for the high spatial, the PMTs and light guides were replaced by a single SiPM array (Hamamatsu S13361), consisting of 64 SiPMs with dimensions of 3x3 mm, arranged into an 8x8 square matrix (see fig 30). A single SiPM therefore can receive light from up to 7 fibres depending on the alignment of a particular SiPM with the fibres.

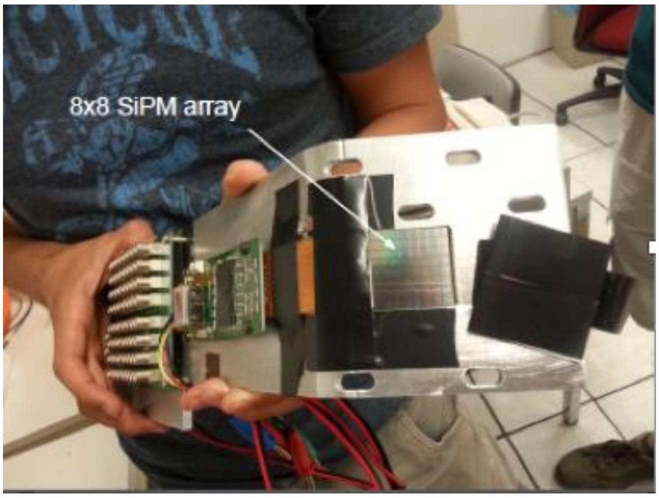

Fig. 30: *SPACAL Setup showing the SiPM array*

Each SiPM consists of 3584 cells with 50µm pitch and has a geometrical fill factor of 74%. The SiPM array can be attached to the SPACAL module at different positions, allowing to collect light from different types of scintillating fibres that are arranged in separate groups within the module.

The SPACAL module with SiPM array attached to it is placed in the thermally isolated metal black box to minimize temperature effects on the gain and dark-current rate of the SiPMs (Fig. 31).

A prototype readout module commercially available from Hamamatsu (C14047-3050EA-08) was used for powering the whole array, as well as amplifying and reading analog signals from each individual SiPM. The CAEN V1742 digitizer was used for digitizing the analog signals at 2.5 GHz sampling frequency.

Taking into account the latency introduced by data transfer from the digitizer, only signals from the central 28 SiPMs was read out to minimise the DAQ dead time and optimise the data-taking efficiency during testbeams.

Two test beam campaigns were performed in H4 beam line of the CERN SPS North Area facility in 2017 and 2018. The SiPM response to an electron, pion and muon beam was studied.

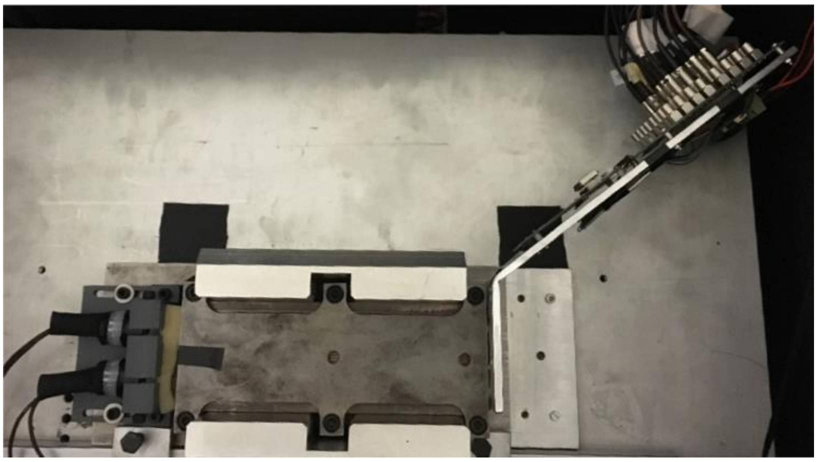

Fig. 31: *Top view of the SPACAL module with 2 PMTs attached on the left and the SiPM array with the readout board attached on the right.*

First measurements with an electron beam showed that the readout board used to amplify the SiPM signals has a power limitation causing the saturation of the amplifier at the signal amplitude of about 110 mV, which significantly reduces the effective dynamic range of the detector prototype. No saturation effects of the SiPM itself were observed during the testbeam. While the amplifier saturation does not allow to properly assess the scintillation light intensity, it is still possible to use the saturated signals as a binary value representing the presence of any scintillation light in a given part of the SPACAL module.

Two hodoscopes were used in the testbeam setup, each providing an independent measurement of the incoming particle position in both horizontal and vertical coordinates. An example of the position sensitivity of such readout is demonstrated in Fig. 30., showing signals from the 28 SiPMs in events with a muon entering the SPACAL module at the particular position as measured by any of the two hodoscopes. The presence of signal in SiPMs distant from the interaction point is caused by the presence of a small air gap (< 2mm) between fibres and SiPM array surface, because the side of the SPACAL module facing the SiPMs is not perfectly flat. This gap allows photons from one fibre to experience multiple reflections from a SiPM and neighbouring fibres reaching more distant parts of the SiPM array.

For evaluation of the spatial resolution of this prototype it is important to use data from minimally ionising particles, like muons or pions. Too little statistics of data was recorded with such beams during the first test beam campaign in 2017. An optimised setup was used in the second test beam campaign in 2018 for minimising the DAQ dead time and recording data of higher relevance for the spatial resolution estimation. In particular, the number of samples recorded by the digitizer was reduced from 1024 to 512, which significantly reduced the time spent on data transfer from the digitizer, while is still enough to verify the presence of scintillation light in a particular SiPM. Also the trigger area was reduced from 3x3 cm to 1x1 cm. It makes the geometrical acceptance smaller given that the area equipped with SiPMs is about 1.5x1.5 cm, but it avoids spending DAQ time on events with the incident particle entering the SPACAL module outside the photodetection area.

Data recorded during the second test beam campaign is still being analysed.

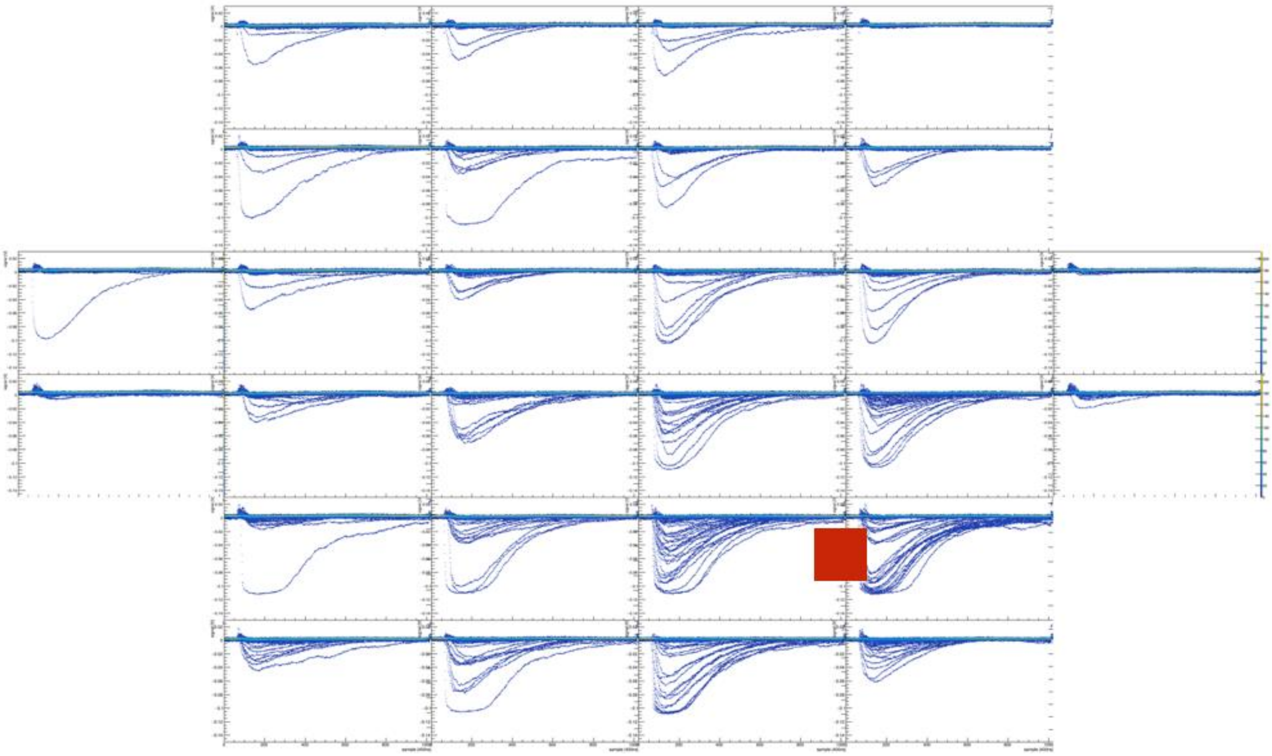

Fig. 31: *Signals from the 28 SiPMs in selected events, where incoming muon position from hodoscopes correcponds to the red square.*

11. CONCLUSION

In the last four years several complementary test stands have been produced and commissioned in different institutes to characterize the optical, the radiation hardness and the performance under high energy particles beam. These different infrastructures have been extensively used in the last years. It has allowed to progress in the understanding of the properties of various types of scintillating fibres and to evaluate the potential of their use in a new concept of calorimetry using SPACAL geometry.

12. REFERENCES

[1] Cova, F. et al. (2018) Radiation hardness of Ce-doped sol-gel silica fibres for High Energy Physics applications, *Opt. Lett.*, 43 (4), 903-906

[2] Cova, F. et al. (2017) Optical properties and radiation hardness of Pr-doped sol-gel silica: Influence of the fibre drawing process, *Journal of Luminescence,* 192, pp 661-667

[3] Auffray, E. et al., (2015) Application of two-photon absorption in PWO scintillator for fast timing of interaction with ionizing radiation, *Nuclear Instruments and Methods in Physics Research, A804, 194–200*

[4] Korjik, M.V. et al. (2016) Non-Linear Optical Phenomena in Detecting Materials as a Possibility for Fast Timing in Detectors of Ionizing Radiation, *IEEE Transactions on Nuclear Science, 60, 2979-2984*

[5] Auffray, E. et al, (2016).Free carrier absorption in self-activated PbWO4 and Ce-doped $Y_3(Al_{0.25}Ga_{0.75})_3O_{12}$ and $Gd_3Al_2Ga_3O_{12}$ garnet scintillators, Optical Materials, 58, 461-465

[6] Auffray, E. et al (2016) Luminescence rise time in self-activated PbWO4 and Ce-doped Gd3Al2Ga3O12 scintillation crystals, *J. Lumin. 178, 54-60*

[7] Tamulaitis, G. et al. (2017) Subpicosecond luminescence rise time in magnesium codoped GAGG:Ce scintillator, *Nuclear Inst. and Methods in Physics Research, A 870, 25–29*

[8] Lucchini, M.T. (2017) Measurement of non-equilibrium carriers dynamics in Ce-doped YAG, LuAG, and GAGG crystals with and without Mg-codoping, *J. Lumin. 194, 1-7*

[9] Smith D R, Hobson P R (2016) Spectrometer Testing: Dark frame evaluation of StellarNet Black Comet spectrometer, Brunel_Spectrometer_Testing_TN_001.01, http://bura.brunel.ac.uk/handle/2438/14089

[10] Marini, A. for the CMS Collaboration (2018) H4DAQ: a modern and versatile data-acquisition package for calorimeter prototypes test-beams, *2018 JINST 13 C02042*

[11] Akchurin, N. et al, (2018) Cerium-doped scintillating fused-silica fibres, J*INST 13, P04010*

[12] Cova, F. et al (2018) Dual Cherenkov and Scintillation Response to High-Energy Electrons of Rare-Earth Doped Silica Fibres, *Phys. Rev. Applied, submitted*

13. ACKNOWLEDGEMENTS

This project has been performed in collaboration with CMS-ECAL and CrystalClear Collaboration. It has received funding from the European Union’s Horizon 2020 Research and Innovation programme AIDA 2020 under Grant Agreement no. 654168 and under the Marie Skłodowska-Curie Intelum grant agreement No 644260 and support for COST ACTION TD1401.